

# Application of Backward Nonlinear Local Lyapunov Exponent Method to Assessing the Relative Impacts of Initial Condition and Model Errors on Local Backward Predictability

Xuan LI<sup>1</sup>, Jie FENG<sup>1</sup>, Ruiqiang DING<sup>\*2</sup>, and Jianping LI<sup>3,4</sup>

<sup>1</sup>*Department of Atmospheric and Oceanic Sciences and Institute of Atmospheric Sciences, Fudan University, Shanghai 200438, China*

<sup>2</sup>*State Key Laboratory of Earth Surface Processes and Resource Ecology, Beijing Normal University, Beijing 100875, China*

<sup>3</sup>*Frontiers Science Center for Deep Ocean Multispheres and Earth System (FDOMES)/Key Laboratory of Physical Oceanography/Institute for Advanced Ocean Studies, Ocean University of China, Qingdao 266100, China*

<sup>4</sup>*Laboratory for Ocean Dynamics and Climate, Pilot Qingdao National Laboratory for Marine Science and Technology (QNLM), Qingdao 266237, China*

(Received 24 December 2020; revised 13 March 2021; accepted 9 April 2021)

## ABSTRACT

Initial condition and model errors both contribute to the loss of atmospheric predictability. However, it remains debatable which type of error has the larger impact on the prediction lead time of specific states. In this study, we perform a theoretical study to investigate the relative effects of initial condition and model errors on local prediction lead time of given states in the Lorenz model. Using the backward nonlinear local Lyapunov exponent method, the prediction lead time, also called local backward predictability limit (LBPL), of given states induced by the two types of errors can be quantitatively estimated. Results show that the structure of the Lorenz attractor leads to a layered distribution of LBPLs of states. On an individual circular orbit, the LBPLs are roughly the same, whereas they are different on different orbits. The spatial distributions of LBPLs show that the relative effects of initial condition and model errors on local backward predictability depend on the locations of given states on the dynamical trajectory and the error magnitudes. When the error magnitude is fixed, the differences between the LBPLs vary with the locations of given states. The larger differences are mainly located on the inner trajectories of regimes. When the error magnitudes are different, the dissimilarities in LBPLs are diverse for the same given state.

**Key words:** Initial condition, model errors, error magnitude, error location, LBPL

**Citation:** Li, X., J. Feng, R. Q. Ding, and J. P. Li, 2021: Application of backward nonlinear local Lyapunov exponent method to assessing the relative impacts of initial condition and model errors on local backward predictability. *Adv. Atmos. Sci.*, **38**(9), 1486–1496, <https://doi.org/10.1007/s00376-021-0434-2>.

## Article Highlights:

- This study introduces a new method to quantify predictabilities of LBPL of specific states with the presence of initial condition or model errors.
- The specific structure of the Lorenz attractor leads to a layered distribution of local backward predictability limits induced by the initial condition or model errors.
- The relative impacts of initial condition and model errors on local backward predictability depend on the locations of given states on the dynamical trajectory and the error magnitudes.

## 1. Introduction

In weather forecasting, two main types of errors affect

the accuracy of forecast results: initial condition errors and model errors. The initial condition errors are the difference between the true and observed values of atmospheric variables. They are unavoidable, no matter how advanced the observation networks or data assimilation methods. In current operational forecasting, numerical models are widely

\* Corresponding author: Ruiqiang DING  
Email: [drq@bnu.edu.cn](mailto:drq@bnu.edu.cn)

used to forecast future states. However, the simplified atmospheric equations, coarse resolution and parameterization schemes introduce model errors in numerical weather prediction. Apart from the initial condition and model errors, the numerical schemes which solve the numerical models will also introduce uncertainty, resulting in loss of predictability (e.g. Gilson et al., 1988; Li et al., 2000; Berner et al., 2009).

Lorenz (1963) pointed out that the chaotic nature of the atmosphere would make slightly differing initial states evolve very differently in phase space over time. Given that the two types of errors can be never eliminated, the atmospheric predictability has an upper limit. Lorenz (1975) classified the problems of atmospheric predictability into two categories. The first predictability is associated with the initial condition errors, while the second predictability is related to the model errors. Researchers have also proposed several methods to quantitatively estimate atmospheric predictability. Early studies attempted to estimate the predictability limit by computing the doubling time of small errors (Leith, 1965; Mintz, 1968; Smagorinsky, 1969). Charney (1966) summarized previous studies and demonstrated that the average doubling time of small errors is 5 days. The Lyapunov exponent (LE) can characterize the average growth rate of chaotic systems, and may be used to quantify atmospheric predictability. However, the LE is almost constant on the attractor (Oseledec, 1968) while predictability is a local property in phase space (Trevisan and Legnani, 1995). Therefore, the LE is not suitable for measuring local predictability. Subsequently, the local LE was proposed to quantify atmospheric predictability (Nese, 1989; Yoden and Nomura, 1993). The local LE method is valid only if the initial error is infinitesimal. Hence, Ding and Li (2007) and Ding et al. (2008) proposed the nonlinear local Lyapunov exponent (NLLE) method to study the nonlinear growth of finite error size in a time interval. Without linearizing the governing equations, they integrated the true state and perturbed state to study the error growth. Therefore, the NLLE method remains applicable even when the initial error grows to a finite size. As an alternative to the NLLE method, Mu et al. (2003) proposed the conditional nonlinear optimal perturbation (CNOP) method to study atmospheric predictability. The CNOP method takes into account the nonlinearity of the atmosphere and can also be used when the initial error grows to a finite size (Mu and Duan, 2003; Duan et al., 2004; Mu and Zhang, 2006; Duan and Mu, 2009). The shadowing property reflects the approximate evolution of a computed trajectory compared to the true one (Sanz-Serna and Larsson, 1993; Vallejo and Sanjuán, 2013). Therefore, the shadowing time can indicate the predictability. Based on the distributions of finite-time LEs, the shadowing time can be calculated. That is, the predictability may be quantified. Recently, Vallejo and Sanjuán (2015) introduced the predictability index to indicate the predictability. The predictability index is also derived from the distributions of finite-time LEs. Since the finite-time LEs are computed by using the tangent linear equations (Yoden and Nomura, 1993; Ding and Li, 2007), the two methods above

are different from the NLLE method. More recently, Daza et al. (2016) has proposed basin entropy to quantify the uncertainties in dynamical systems. Basin entropy has proven to be an effective method for study of the mechanism of loss of predictability in several paradigmatic models. It is essential to introduce this method into the predictability of extreme weather events in the future.

These methods allow us to estimate the prediction time within which weather forecasts are credible. However, the general public and policymakers are often more concerned with the prediction lead time of specific weather events such as extreme heat waves or heavy rainfall that can cause socioeconomic damage. The predictability of extreme weather events is different from that of normal weather events. To distinguish the predictability of specific weather events from that of normal weather events, Li et al. (2019) proposed two new notions of predictability: the local forward and local backward predictabilities. The local forward predictability is associated with the prediction time of normal weather events, while the local backward predictability is concerned with the maximum prediction lead time of extreme weather events. In current operational forecasts, owing to some uncertainties present in the observations and models, forecasts in the first few days are sufficiently accurate to inform the public well. Questions arise as to whether the accurate forecast time can be extended, and how to determine the upper predictability limit from initial normal events, but these questions are unsolved. Though two weeks are widely recognized as the upper limit, this problem still needs more intensive examination. In order to address this problem, Li et al. (2019) introduced the notion of local forward predictability to study the upper predictability limit from initial normal states. Since extreme weather events occur at a low frequency, their predictabilities are unique and differ from those of normal weather events (Mu et al., 2002; Chou, 2011). It is more difficult to estimate the predictability of extreme weather events. In order to estimate the predictability of extreme weather events, Li et al. (2019) indicated that the growing forecast errors resulting in such events should be analyzed, and proposed the notion of local backward predictability to study these kinds of events. Hence, the forward and backward predictabilities are focused on different kinds of weather events. Li et al. (2020b) studied the relative roles of initial condition and model errors in local forward predictability in the Lorenz model and found that the initial condition errors are more dominant in the forward predictability than model errors, consistent with previous studies (e.g. Downton and Bell, 1988; Lorenz, 1989; Richardson, 1998). The complexity of the predictability of specific weather events has meant that there are very few relevant studies on the relative roles of the two types of errors in local backward predictability. The occurrence of specific states, especially extreme states, has a greater impact on human society, so it is necessary to study the relative effects of the two types of errors on the local backward predictability of specific states, which may provide theoretical guidance for improving forecast skill. Ding and Li (2007) introduced the

NLLE method to quantify the maximum prediction time from a random initial state. However, this technique can't quantify how much time a specific state can be predicted in advance. In order to address this problem, Li et al. (2019) developed the backward nonlinear local Lyapunov exponent (BNLLE) method on the basis of the NLLE technique. By calculating the time of forecast errors growing to saturation level from the corresponding initial state to the specific state, the local predictability of the specific state can be quantified. Therefore, the NLLE and BNLLE techniques have different research objects. The NLLE method has been widely used in the atmospheric predictability or related fields (e.g., Li and Ding, 2013; He et al., 2021). However, since the BNLLE method was introduced, it has just been applied to a single study comparing the predictabilities of warm and cold events (Li et al., 2020a). In the present work, we will perform a theoretical study to investigate the relative effects of initial condition and model errors on the local backward predictability of specific states based on the BNLLE method. The BNLLE method is used to quantify the local backward predictability limit (LBPL) of a specific state. Therefore, the relative effects of initial condition and model errors on local backward predictability can be quantitatively estimated by comparing the difference between the LBPLs. The remainder of this paper is organized as follows. Section 2 introduces the BNLLE method and Lorenz model. The results of quantitative comparisons of the relative effects of initial condition and model errors on local backward predictability are presented in section 3. Finally, a discussion and conclusions are given in section 4.

## 2. Model and method

### 2.1. Model description

In this work, the Lorenz model (1963, hereafter referred to as Lorenz63 model) is used to investigate the relative impacts of two types of uncertainties on local backward predictability. The Lorenz63 model is a conceptual model of the real atmosphere and has been widely used in studies of atmospheric predictability (e.g. Palmer, 1993; Evans et al., 2004; He et al., 2006, 2008; Feng et al., 2014; Li et al., 2020a). The detailed description of model setup parallels that of Li et al. (2020b).

### 2.2. BNLLE method

Ding and Li (2007) proposed the NLLE method to quantitatively estimate atmospheric predictability. Figure 1 shows the mean local relative error growth of initial errors as a function of time for different error magnitudes in the Lorenz63 model. The initial errors grow with a regularly oscillating pattern at the early stage. After that, the errors reach a saturation level and cease to grow. For different magnitudes of initial error, the time to reach saturation is different. Smaller initial errors take more time to reach saturation. Before the saturation stage, the errors grow in the linear regime. When the errors are in the period of saturation, the nonlinearity domin-

ates the error growth (e.g. Lacarra and Talagrand, 1988; Farrell, 1990; Lorenz, 2005). Therefore, the local forward predictability limit of a single state in phase space can be measured as the time when the forecast error exceeds 95% of the saturation value (Li et al., 2019).

Using the NLLE algorithm, we can obtain the local forward predictability limit of any initial state. However, we cannot estimate the LBPL of a given state, especially for the extreme states that are of greater interest. On the basis of the NLLE algorithm, Li et al. (2019) introduced an algorithm, BNLLE, for estimating the LBPL of a given state. In an  $n$ -dimensional system, the growth of small errors  $\delta(t_0)$  perturbed on the initial state  $\mathbf{x}(t_0)$  can be expressed by

$$\delta(t_0 + \tau) = \eta(\mathbf{x}(t_0), \delta(t_0), \tau) \delta(t_0), \quad (1)$$

where  $\eta(\mathbf{x}(t_0), \delta(t_0), \tau)$  is the nonlinear error propagator, and the  $\delta(t_0 + \tau)$  is the time-dependent error at time  $t_0 + \tau$ . The average growth rate of errors, also called the NLLE (Ding and Li, 2007) can be described by

$$\lambda(\mathbf{x}(t_0), \delta(t_0), \tau) = \frac{1}{\tau} \ln \frac{\|\delta(t_0 + \tau)\|}{\|\delta(t_0)\|}, \quad (2)$$

where  $\lambda(\mathbf{x}(t_0), \delta(t_0), \tau)$  represents the average growth rate of errors. Therefore, the average growth of forecast errors varying with time can be obtained (shown in Fig. 1). Based on the saturation time of forecast errors, we can estimate the local forward predictability limit of state  $\mathbf{x}(t_0)$ . Li et al. (2019) pointed out that a specific state has a corresponding initial state. In order to estimate the LBPL of a specific state, the corresponding initial state must be found first. Once the corresponding initial state is determined, then the time length between the corresponding initial state and specific state is defined as the LBPL of the specific state. Li et al. (2019, 2020a) indicated that if numerous infinitesimal small errors perturbed on the state  $\mathbf{x}(t_0)$  grow to saturation level at the time of the specific state, the state  $\mathbf{x}(t_0)$  is the cor-

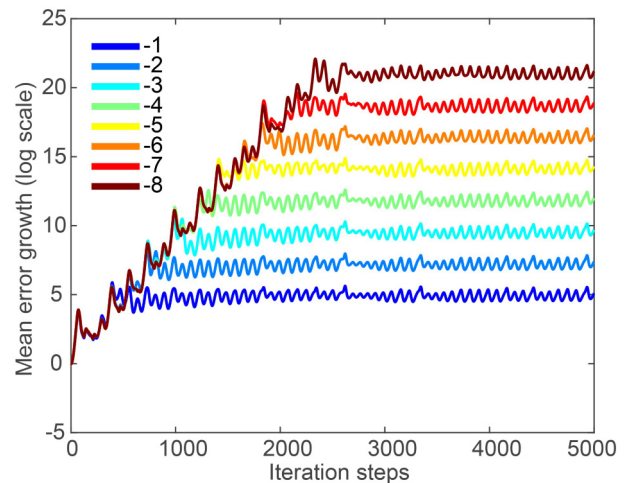


**Fig. 1.** Mean growth of initial errors with different magnitudes ( $\log_{10}$  scale), for magnitudes of  $10^{-1}$ ,  $10^{-2}$ ,  $10^{-3}$ ,  $10^{-4}$ ,  $10^{-5}$ ,  $10^{-6}$ ,  $10^{-7}$ , and  $10^{-8}$ . The mean error growths are given in terms of natural logarithms (base  $e$ ).

responding initial state. Considering that the predictability of the specific state is estimated by repeating a backward search for the corresponding initial state, the technique is called BNLLE (Li et al., 2019).

Figure 2 shows the simple procedure for determining the LBPL of the given state  $\mathbf{x}(t_n)$ . The state  $\mathbf{x}(t_n)$  is a large value of the climate variables in the time series data  $[\mathbf{x}(t_1), \mathbf{x}(t_2), \dots, \mathbf{x}(t_n), \dots]$ . Based on the BNLLE method, the state at time  $t_m$  is the corresponding initial state. Therefore, the prediction lead time of state  $\mathbf{x}(t_n)$  can be quantitatively estimated  $(t_n - t_m)$ . Li et al. (2020a) has applied the BNLLE method to compare backward predictabilities of warm and cold events in the Lorenz63 model and found that the warm events are more predictable.

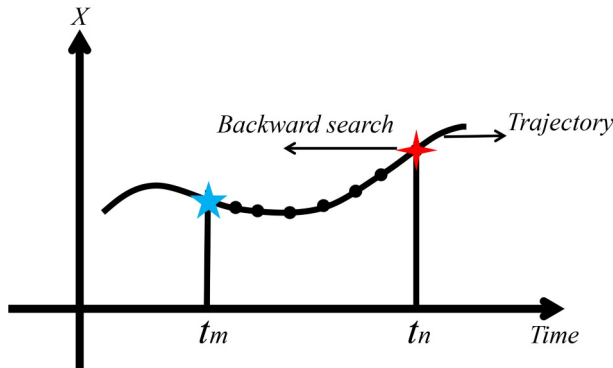


**Fig. 2.** Schematic of the algorithm used to estimate the LBPL of given state  $\mathbf{x}(t_n)$ . The vertical axis represents climate variables  $X$ , and the horizontal axis represents the evolution time of  $X$ . The solid curve shows the variation of climate variables  $X$  over time. The red diamond-shaped star is the given state at time  $t_n$ . The blue star represents the corresponding initial state at time  $t_m$  that is being searched for. The black solid points on the trajectory are intermediate states.

### 3. Results

#### 3.1. Scenario one: Only initial condition errors

To investigate the effects of initial condition errors on the local backward predictability of given states, the model should be perfect. If  $(\mathbf{x}(t_0), \mathbf{y}(t_0), \mathbf{z}(t_0))$  is a true state, then the imperfect initial state  $(\mathbf{x}'(t_0), \mathbf{y}'(t_0), \mathbf{z}'(t_0))$  can be obtained by superimposing the initial error vector  $\delta$  on the true state.

$$\mathbf{x}'(t_0) = \mathbf{x}(t_0) + \delta_1, \quad (3)$$

$$\mathbf{y}'(t_0) = \mathbf{y}(t_0) + \delta_2, \quad (4)$$

$$\mathbf{z}'(t_0) = \mathbf{z}(t_0) + \delta_3, \quad (5)$$

$$\delta^2 = \delta_1^2 + \delta_2^2 + \delta_3^2. \quad (6)$$

Here  $\delta_1$ ,  $\delta_2$ , and  $\delta_3$  are small perturbations superimposed on the three variables of Lorenz63 model. In this work, the number of random initial error vectors is 10 000 and their magnitudes are both  $10^{-5}$ . The Lorenz attractor has warm and cold regimes, and regions on the regime transitions are dynamically unstable (Evans et al., 2004). Therefore, we chose an initial state  $(-0.46, 5.02, 30.90)$  for the dynamically unstable region. From this initial state, another 1999 consecutive states on the same trajectory were also chosen. Based on the BNLLE method, the LBPLs of 2000 consecutive states were calculated.

Figure 3 shows the spatial distribution of the LBPLs of these consecutive states. The figure shows two unstable stationary points,  $(\sqrt{\beta(r-1)}, \sqrt{\beta(r-1)}, r-1)$  and  $(-\sqrt{\beta(r-1)}, -\sqrt{\beta(r-1)}, r-1)$ , located at the center of the two regimes (Mukougawa et al., 1991; Mu et al., 2002). On

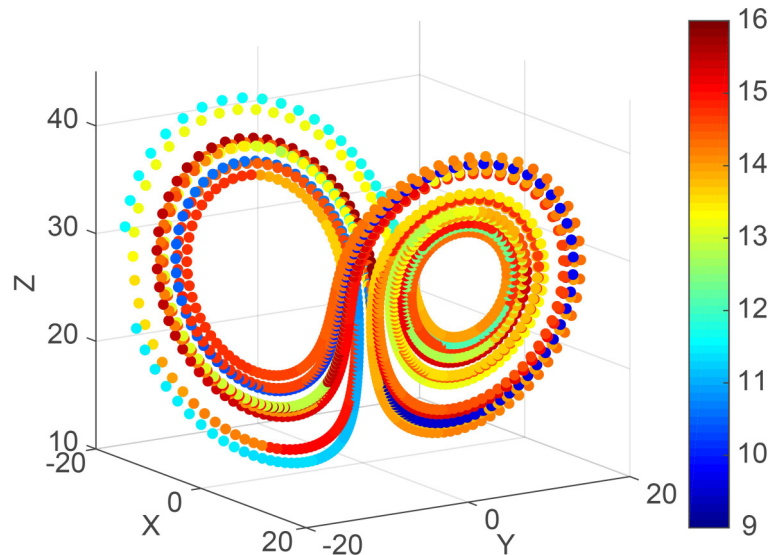


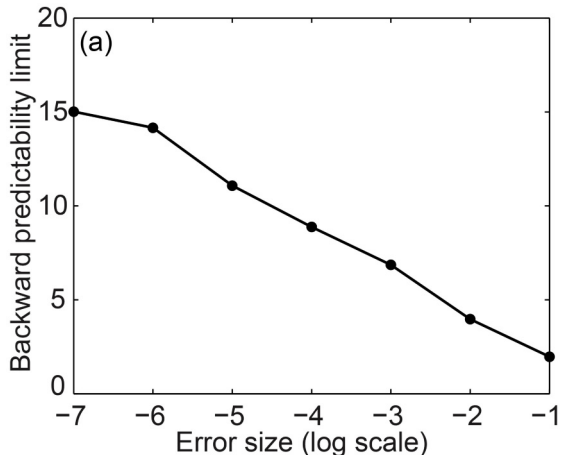
**Fig. 3.** Spatial distribution of LBPLs for 2,000 consecutive initial conditions from the given state  $(-0.46, 5.02, 30.90)$  on the Lorenz attractor.

every individual circular orbit around the unstable stationary points, the LBPLs of the given states are almost the same. For different circular orbits, the LBPLs are different. Therefore, the LBPLs of given states present obvious layered structures, which is consistent with the results of Li et al., (2020b). The physical reason for the layered structures may originate from the specific spatial structure of the Lorenz attractor. The physical properties of each individual circular orbit around the unstable stationary point are the same. Therefore, each given state on the individual circular orbit has almost the same predictability. Different circular orbits have different locations in phase space, leading to varying predictabilities (Nese, 1989; Trevisan and Legnani, 1995).

We also investigated the effects of the magnitude of initial condition errors on the LBPLs of given states. In order to make the conclusion more robust, the selected states should have different dynamical properties. We selected two states  $[(-0.61, 2.66, 28.49) \text{ and } (-3.87, -5.69, 18.00)]$ , the former of which is located in the dynamically unstable region, while the latter is located in the cold regime. Thus, they represent different dynamical flows and have different dynamical properties. The LBPLs of the two given states (Fig. 4) reveal that the LBPLs decrease as the size of the initial condition errors increases. For different given states, initial condition errors of the same size have different influences. When the magnitude of the initial condition errors is  $10^{-7}$ , the LBPLs of  $(-0.61, 2.66, 28.49)$  is 15 time units, while that of  $(-3.87, -5.69, 18.00)$  is 19 time units. For other error magnitudes, the LBPLs are also different. This is because the local backward predictabilities depend on the given state on the dynamical trajectory. The two given states are on different locations of the dynamical flows, and the predictability varies with location; consequently, the LBPLs of the two given states are different, although the magnitudes of the initial condition errors superposed on them are the same.

### 3.2. Scenario two: Only model errors

For the scenario of model errors without initial errors,



the model is imperfect. Likewise, we perturbed three parameters with small perturbations in the Lorenz63 model.

$$\sigma' = \sigma + \varepsilon_1, \quad (7)$$

$$b' = b + \varepsilon_2, \quad (8)$$

$$r' = r + \varepsilon_3, \quad (9)$$

$$\varepsilon^2 = \varepsilon_1^2 + \varepsilon_2^2 + \varepsilon_3^2. \quad (10)$$

Here  $\varepsilon_1$ ,  $\varepsilon_2$ , and  $\varepsilon_3$  are small perturbations superimposed on the three parameters. The given states are the same 2000 consecutive states as used above. Using the BNLLE method, we can estimate the LBPLs of these states induced by 10 000 random model errors with magnitude of  $10^{-5}$ .

Figure 5 shows the spatial distribution of LBPLs of the 2000 consecutive states; the LBPLs induced by model errors also show layered structures similar to those induced by initial condition errors. It is the specific structure of the Lorenz attractor determines the specific spatial distributions of the LBPLs. Therefore, the above results indicate that structure of the attractor has greater effects on predictability limits and their distributions. We also investigate the effects of model error magnitude on the LBPLs of given states. The situation is the same as for initial condition errors (shown in Fig. 6). Increasing the model error magnitude reduces the LBPLs of given states. The LBPLs of different given states are different, although the model error magnitudes are the same.

### 3.3. Relative effects of initial condition and model errors

The existence of initial condition and model errors affects the predictability, which leads to an upper limit. To quantify the relative effects of initial condition and model errors on the local backward predictability of given states, we compare the LBPLs they induce. In the case when the LBPLs of the given state induced by initial condition errors

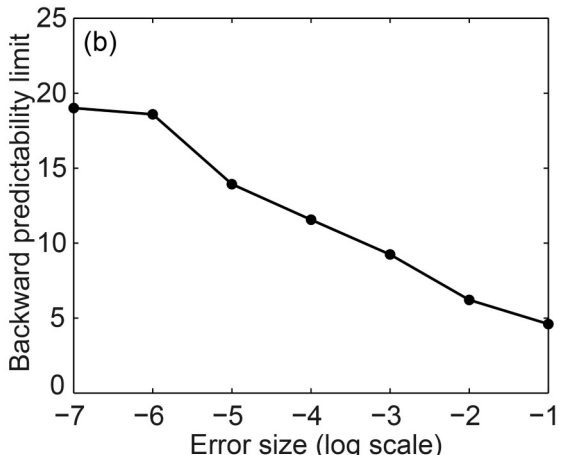


**Fig. 4.** Variation of LBPLs for initial condition errors for given states (a)  $(-0.61, 2.66, 28.49)$  and (b)  $(-3.87, -5.69, 18.00)$ . Error size is shown on a  $\log_{10}$  scale.

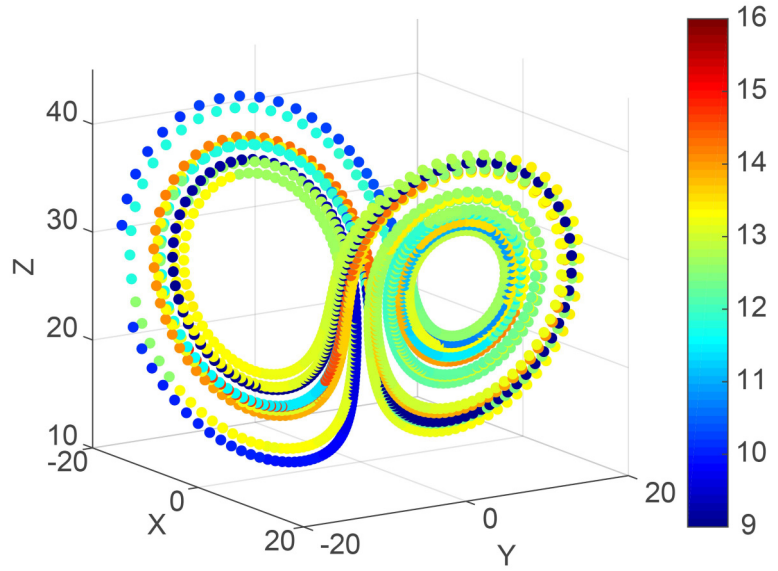


**Fig. 5.** Same as Fig. 3, but for the model error.

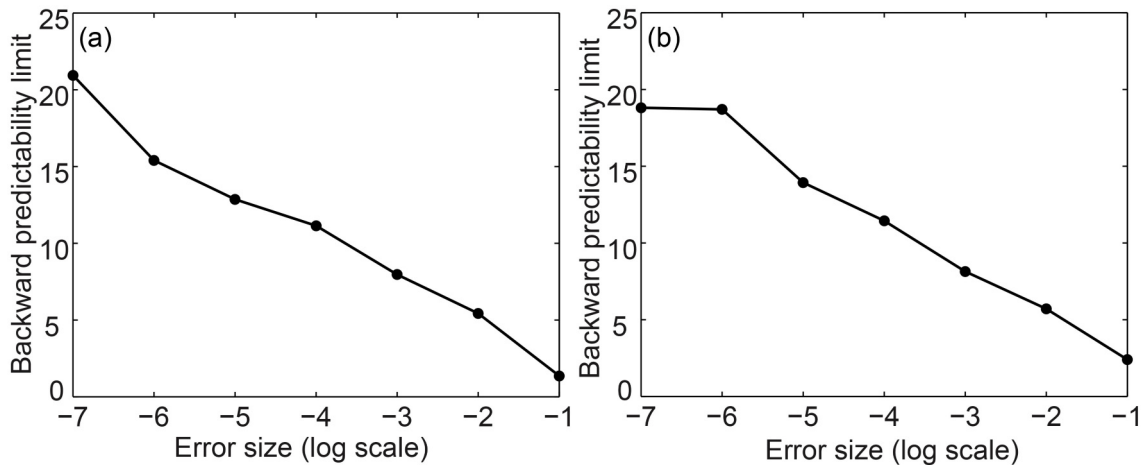


**Fig. 6.** Same as Fig. 4, but for the model error.

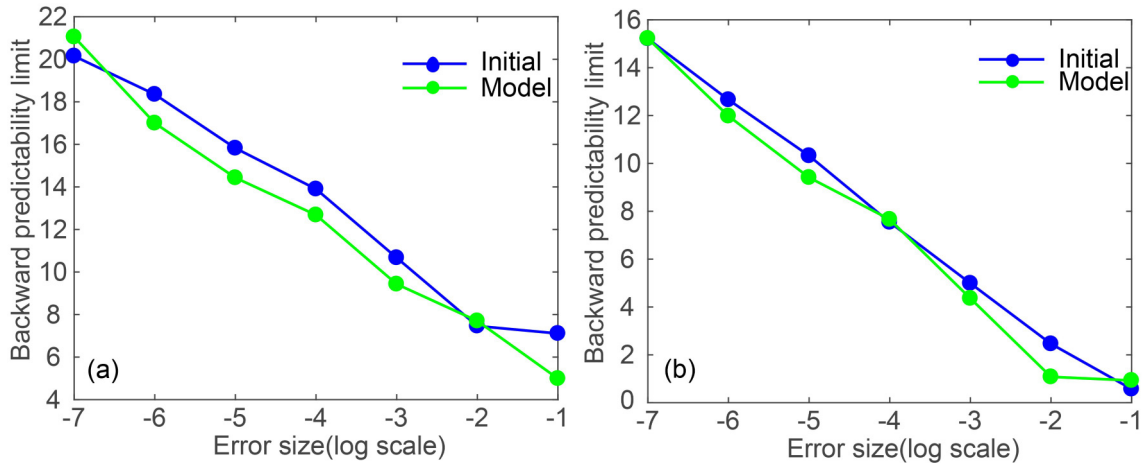


**Fig. 7.** Variation of LBPLs for the two types of errors for the states (a)  $(-0.54, 1.88, 26.43)$  and (b)  $(-0.32, 1.27, 24.64)$ . Error size is given on a  $\log_{10}$  scale.

are higher than those of the same given state induced by model errors, this indicates that model errors have a larger impact, resulting in a lower local predictability limit, and vice versa. [Figure 7](#) shows the variation of the LBPLs of two given states with the magnitude of the two types of errors. In [Fig. 7a](#), for the given state  $(-0.54, 1.88, 26.43)$  and an error magnitude of  $10^{-7}$ , the LBPLs induced by model errors are slightly higher than those induced by initial condition errors. This demonstrates that initial condition errors have a greater influence on LBPLs, resulting in lower predictability. When the error magnitude is  $10^{-2}$ , the LBPLs induced by the two types of errors are roughly the same, so the initial condition and model errors have the same effects on local backward predictability. For other error magnitudes, the LBPLs induced by model errors are lower, indicating model errors have more influence. Therefore, when error magnitudes are different, the relative roles of initial condition and model errors in LBPLs vary. In [Fig. 7b](#), when the error magnitude is  $10^{-7}$ , the LBPLs induced by the two types of errors are both 15, unlike the case for the given state  $(-0.54, 1.88, 26.43)$  in [Fig. 7a](#). With other magnitudes, the situation is the same, with the relative importance of the two types of errors being different from those at the first given state. The two previous initial states were also analyzed (figures not shown). The conclusion is similar to that of the two new initial states. Therefore, even though the same error magnitude may be superimposed, if the given states are different, then the relative effects of the two types of errors are different. This indicates that the relative roles of initial condition and model errors depend on the position of the given states on the dynamical trajectory in phase space.

To verify this conclusion, we selected more states to analyze. Considering that the previous 2000 consecutive states originated from the dynamically unstable regions, they are

appropriate to use in the following analysis. [Figure 8](#) shows the LBPLs induced by the two types of errors and their difference as a function of the number of states for up to 2000 states. [Figure 8a](#) shows that the LBPLs induced by initial condition and model errors have the same tendencies independent of error magnitude. As the number of specified states increases, the LBPLs first increase monotonically, then decrease monotonically, with the pattern repeating with increasing number of states. In [Fig. 8b](#), when the magnitudes of initial condition and model errors are both  $10^{-2}$  (red solid and dashed lines), the differences between model error and initial error of LBPLs are positive for the first 1339 given states, so model errors play a greater part in local backward predictability than initial condition errors, resulting in lower LBPLs. The differences are negative for the remaining 661 states, for which the initial condition errors have a greater influence on local backward predictability. Thus, the relative effect of initial condition and model errors varies with the specified state. [Figure 8b](#) also shows that the differences between the LBPLs of the same given states are different when the error magnitudes are different. This demonstrates that the error magnitude affects the relative effects of initial condition and model errors on local backward predictability.

[Figure 9](#) shows the spatial distributions of LBPLs of previous 2000 consecutive states induced by the two types of errors and their differences. On an individual circular orbit, the LBPLs of given states are roughly the same, whereas the LBPLs of given states on the regime transitions are different. From the warm (cold) regime to the cold (warm) regime, the properties of states change, resulting in different predictabilities in the regime transition region. When the error magnitude is  $10^{-2}$ , the LBPLs of the 1336 states induced by initial condition errors are higher than those of the remaining states induced by model errors. For most of

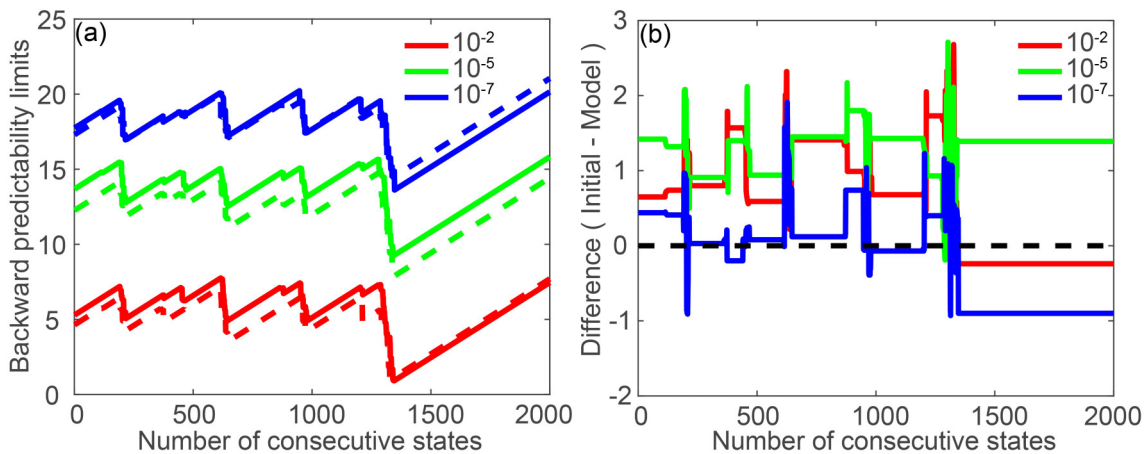


**Fig. 8.** (a) LBPLs of 2,000 consecutive states induced by initial and model errors with different magnitudes. (b) Difference (initial condition errors minus model errors) of LBPLs induced by initial and model errors of these consecutive states with different magnitudes. The solid and dashed lines in (a) represent LBPLs induced by initial condition and model errors, respectively. The red, green, and blue solid or dashed lines refer to error magnitudes of  $10^{-2}$ ,  $10^{-5}$ , and  $10^{-7}$ , respectively (as shown by  $\log_{10}$  values  $-2$ ,  $-5$ , and  $-7$ ). The black dashed line in (b) is the zero value.

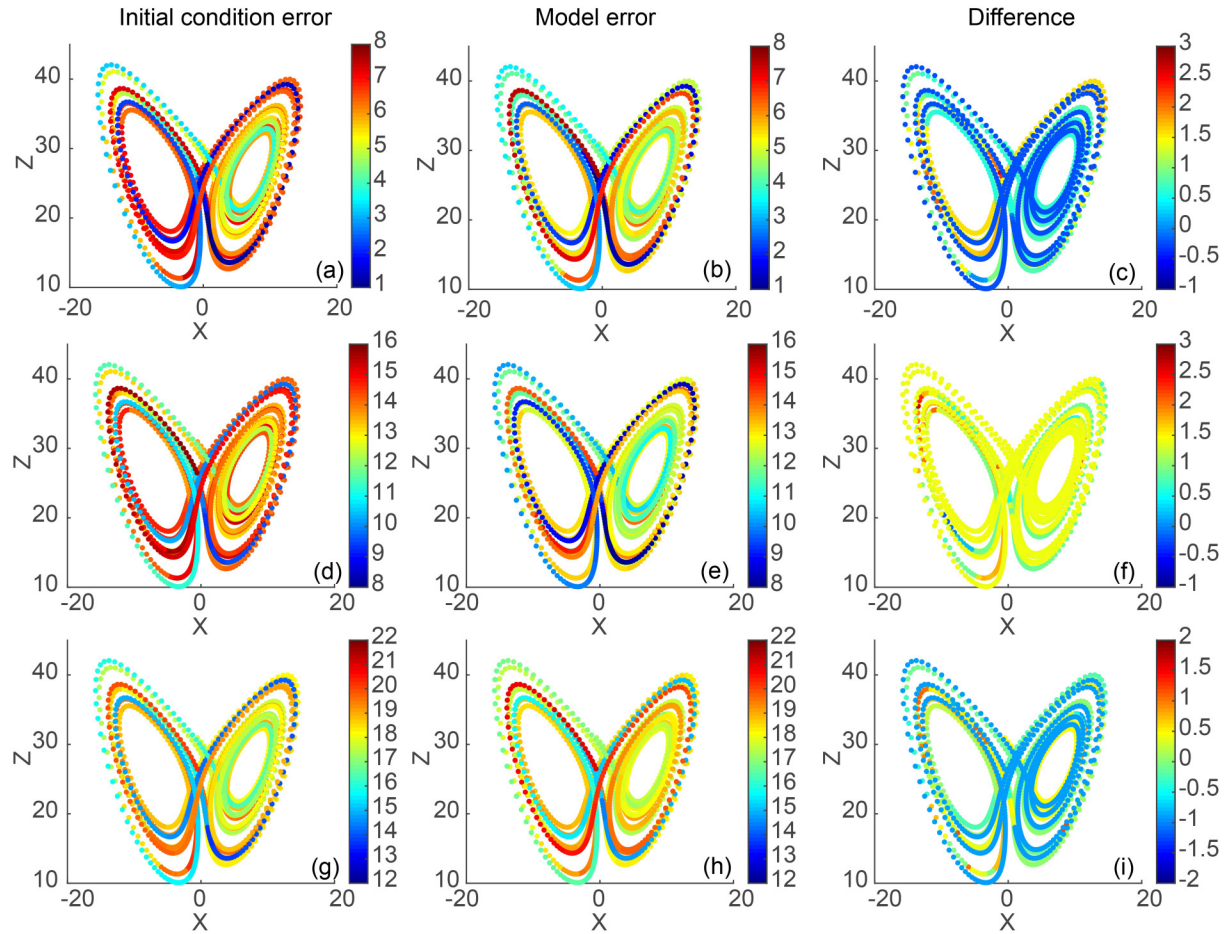


**Fig. 9.** Spatial distributions of LBPLs projected on the  $X$ - $Z$  plane of the Lorenz attractor with initial condition and model error magnitudes of (a–c)  $10^{-2}$ , (d–f)  $10^{-5}$ , and (g–i)  $10^{-7}$ . The left panels only have initial condition errors in the system, the middle panels only have model errors, and the right panels show the differences between the LBPLs (initial condition errors minus model errors) induced by initial condition and model errors.

these 1336 states, the differences in the predictabilities are only slightly larger than zero, with just a small minority having larger values of up to nearly 3 time units. The large values in the local predictability difference of states are mainly distributed on the inner trajectories of the left regime. When the magnitude of errors is  $10^{-5}$ , the large values of difference are spread all over the attractor. When the magnitude of errors is  $10^{-7}$ , the large differences are found on the inner trajectories of both regimes. Therefore, the inner trajectories of left regime are frequent regions where the model errors have a larger impact on local backward predictability. But on other regions of the attractor, the initial condition errors play a more important role in local backward predictability. This also demonstrates that the relative effects of initial condition and model errors vary with the spatial locations of given states in phase space. From the spatial distributions, for the same given state with different error magnitudes, the difference between the LBPLs is not the same. This further demonstrates that the relative effects depend on the error magnitudes.

#### 4. Conclusions and discussion

Initial condition and model errors are two main contributors to the loss of atmospheric predictability. Based on these sources of errors, Lorenz (1975) classified the predictability into two types: the first associated with initial condition errors and the second driven by model errors. Initial condition errors are unavoidable in observations, while model errors are due to imperfect knowledge of atmospheric motions, coarse resolution, numerical schemes and so on (e.g. Vannitsem and Toth, 2002). It is essential to investigate which type of error has the larger impact on predictability, so that operational forecast skills may then be improved significantly by attempting to reduce that error. This issue has been studied intensely but no consensus has been reached. There have also been fewer studies aimed at the predictability limits of specific weather events and the relative roles of the two types of errors in their predictability.

The general public and policymakers are more focused on how long in advance specific, high-impact weather events can be forecasted compared with normal weather events. Moreover, considering the rare occurrence of spe-

cific weather events, their predictabilities are unique and differ from those of normal weather events and current predictability methods fail to estimate their prediction lead time. To investigate the predictability of specific states, [Li et al. \(2019\)](#) proposed the BNLLE method to quantitatively estimate the LBPLs (maximum prediction lead time) of specific states.

In this work, based on the BNLLE method, we performed a theoretical study with the Lorenz model to investigate the relative effects of initial condition and model errors on the LBPLs of given states. For both types of errors, the LBPLs of given states present obvious layered structures. That is, the LBPLs of given states are roughly the same on an individual circular orbit, and are different on different circular orbits. A possible explanation of this result is that the physical properties of states on an individual circular orbit are the same, resulting in the same LBPLs. As local predictability varies with location in phase space, the LBPLs are different on different circular orbits. We also find that the local backward predictability depends on the error magnitude. For a given state, the LBPLs vary with the superimposed error magnitude. The LBPLs decrease as the magnitudes of the initial condition or model errors increase. The same magnitude of initial condition or model errors may result in different LBPLs of different given states.

Next, we compared the relative effects of initial condition and model errors on the local backward predictability of consecutive states. In the case that the difference between the LBPLs induced by initial condition and model errors is positive, our results indicate that model errors have a larger influence on local backward predictability, resulting in lower LBPLs, and vice versa. We chose 2000 consecutive states on the Lorenz attractor and calculated their LBPLs. On the whole, the differences are not always positive or always negative, indicating that the relative roles of initial condition and model errors in LBPLs vary from state to state on the dynamical trajectory. With a magnitude of  $10^{-2}$ , the larger differences are mainly located on the inner trajectory of the left regime. With a magnitude of  $10^{-5}$ , the larger differences are spread all over the attractor. With a magnitude of  $10^{-7}$ , the larger differences are distributed on the inner orbits of both regimes. Therefore, the inner trajectories of left regime are frequent regions where the model errors have a larger impact on local backward predictability. From the spatial distribution of LBPLs, it further demonstrates the importance of error magnitudes in the relative effects of initial condition and model errors on the local backward predictability.

From the results, the impacts of model errors are not always larger or smaller than those of initial condition errors. This is because different dynamical regions are located on the Lorenz attractor. Some regions are more sensitive to the model errors. In these regions, model errors perturbed on the states grow more rapidly, resulting in larger contributions to the loss of predictability. For different magnitudes of errors, model errors always have impacts on the

inner trajectories of left regime, indicating its sensitivity to model errors. Equally, some dynamical regions are more sensitive to the initial condition errors, resulting in larger impacts on the predictability. Therefore, the results inform us that numerical weather and climate prediction models may improve prediction skills by determining the sensitive regions and reducing the corresponding errors. [Lorenz \(1963\)](#) pointed out that the chaotic systems were sensitive to the initial conditions. Slight differences between the two adjacent initial conditions will grow rapidly over time. Therefore, forecast errors in operational forecast are dependent on the initial conditions. However, the initial condition is not the only factor to influence the growth of forecast errors. The model errors, numerical schemes and some other sources will also influence the growth of forecast errors. In this work, we studied the impacts of model errors on the forecast error growth in the absence of initial condition errors. The findings indicate that for some cases, the model errors play a more important role in the forecast error growth. Under such circumstances, the effects of model errors on the saturation value or the limit cannot be ignored.

Although numerical models are widely used in the study of predictability, theoretical predictability methods are still necessary. The predictability limits estimated by theoretical predictability methods are complementary to those estimated by numerical models. Some research has succeeded in applying theoretical predictability methods to estimate the potential predictability limits of the real atmosphere based on observational data (e.g. [Ding et al., 2010, 2015; Li and Ding, 2011](#)). In the present work, we applied the BNLLE method using a simple theoretical model. It is our view that it is first necessary to further examine the performance of the new method BNLLE. Only if the BNLLE performs well in the simple mode, will we have confidence to apply it to more sophisticated models. In addition, this study sheds light on the relative contributions of two types of errors on local predictability of specific states, which is also beneficial to estimating the predictability of extreme events in more sophisticated models. Therefore, it is important to carry on this work. Nevertheless, the BNLLE method applied to estimating the local backward predictability of specific states in the Lorenz model is a preliminary attempt. In the future, we will apply the BNLLE method to estimate the LBPLs of extreme weather events in the real atmosphere, which may provide guidance to modelers.

**Acknowledgments.** This work was jointly supported by the National Natural Science Foundation of China (Grant Nos. 42005054, 41975070) and China Postdoctoral Science Foundation (Grant No. 2020M681154).

## REFERENCES

Berner, J., G. J. Shutts, M. Leutbecher, and T. N. Palmer, 2009: A spectral stochastic kinetic energy backscatter scheme and its impact on flow-dependent predictability in the ECMWF ensemble prediction system. *J. Atmos. Sci.*, **66**(3), 603–626,

<https://doi.org/10.1175/2008JAS2677.1>.

Charney, J. G., 1966: The feasibility of a global observation and analysis experiment. *Bull. Amer. Meteor. Soc.*, **47**, 200–221, <https://doi.org/10.1175/1520-0477-47.3.200>.

Chou, J. F., 2011: Predictability of weather and climate. *Advances in Meteorological Science and Technology*, **1**(2), 11–14. (in Chinese with English abstract)

Daza, A., A. Wagemakers, B. Georgeot, D. Guéry-Odelin, and M. A. F. Sanjuán, 2016: Basin entropy: A new tool to analyze uncertainty in dynamical systems. *Scientific Reports*, **6**(1), 31416, <https://doi.org/10.1038/srep31416>.

Ding, R. Q., and J. P. Li, 2007: Nonlinear finite-time Lyapunov exponent and predictability. *Physics Letters A*, **364**, 396–400, <https://doi.org/10.1016/j.physleta.2006.11.094>.

Ding, R. Q., J. P. Li, and H. Kyung-Ja, 2008: Nonlinear local Lyapunov exponent and quantification of local predictability. *Chinese Physics Letters*, **25**, 1919–1922, <https://doi.org/10.1088/0256-307X/25/5/109>.

Ding, R. Q., J. P. Li, and K. H. Seo, 2010: Predictability of the Madden-Julian oscillation estimated using observational data. *Mon. Wea. Rev.*, **138**, 1004–1013, <https://doi.org/10.1175/2009MWR3082.1>.

Ding, R. Q., J. P. Li, F. Zheng, J. Feng, and D. Q. Liu, 2015: Estimating the limit of decadal-scale climate predictability using observational data. *Climate Dyn.*, **46**, 1563–1580, <https://doi.org/10.1007/s00382-015-2662-6>.

Downton, R. A., and R. S. Bell, 1988: The impact of analysis differences on a medium range forecast. *Meteor. Mag.*, **117**, 279–284.

Duan, W. S., and M. Mu, 2009: Conditional nonlinear optimal perturbation: Applications to stability, sensitivity, and predictability. *Science in China Series D: Earth Sciences*, **52**, 883–906, <https://doi.org/10.1007/s11430-009-0090-3>.

Duan, W. S., M. Mu, and B. Wang, 2004: Conditional nonlinear optimal perturbations as the optimal precursors for El Niño-Southern Oscillation events. *J. Geophys. Res.*, **109**, D23105, <https://doi.org/10.1029/2004JD004756>.

Evans, E., N. Bhatti, J. Kinney, L. Pann, M. Peña, S. C. Yang, E. Kalnay, and J. Hansen, 2004: RISE undergraduates find that regime changes in Lorenz's model are predictable. *Bull. Amer. Meteor. Soc.*, **85**, 520–524, <https://doi.org/10.1175/BAMS-85-4-520>.

Farrell, B. F., 1990: Small error dynamics and the predictability of atmospheric flows. *J. Atmos. Sci.*, **47**, 2409–2416, [https://doi.org/10.1175/1520-0469\(1990\)047<2409:SED-ATP>2.0.CO;2](https://doi.org/10.1175/1520-0469(1990)047<2409:SED-ATP>2.0.CO;2).

Feng, J., R. Q. Ding, D. Q. Liu, and J. P. Li, 2014: The application of nonlinear local Lyapunov vectors to ensemble predictions in Lorenz systems. *J. Atmos. Sci.*, **71**, 3554–3567, <https://doi.org/10.1175/JAS-D-13-0270.1>.

Gilson, M. K., K. A. Sharp, and B. H. Honig, 1988: Calculating the electrostatic potential of molecules in solution: Method and error assessment. *Journal of Computational Chemistry*, **9**(4), 327–335, <https://doi.org/10.1002/jcc.540090407>.

He, W.-P., G.-L. Feng, W.-J. Dong, and J.-P. Li, 2006: On the predictability of the Lorenz system. *Acta Physica Sinica*, **55**, 969–977, <https://doi.org/10.3321/j.issn:1000-3290.2006.02.088>. (in Chinese with English abstract)

He, W. P., G. L. Feng, Q. Wu, S. Q. Wan, and J. F. Chou, 2008: A new method for abrupt change detection in dynamic structures. *Nonlinear Processes in Geophysics*, **15**, 601–606, <https://doi.org/10.5194/npg-15-601-2008>.

He, W. P., X. Q. Xie, Y. Mei, S. Q. Wan, and S. S. Zhao, 2021: Decreasing predictability as a precursor indicator for abrupt climate change. *Climate Dyn.*, <https://doi.org/10.1007/s00382-021-05676-1>.

Lacarra, J. F., and O. Talagrand, 1988: Short-range evolution of small perturbations in a barotropic model. *Tellus A: Dynamic Meteorology and Oceanography*, **40**, 81–95, <https://doi.org/10.3402/tellusa.v40i2.11784>.

Leith, C. E., 1965: Numerical simulation of the earth's atmosphere. *Methods in Computational Physics*, **4**, 1–28.

Li, J. P., and R. Q. Ding, 2011: Temporal-spatial distribution of atmospheric predictability limit by local dynamical analogs. *Mon. Wea. Rev.*, **139**, 3265–3283, <https://doi.org/10.1175/MWR-D-10-05020.1>.

Li, J. P., and R. Q. Ding, 2013: Temporal-spatial distribution of the predictability limit of monthly sea surface temperature in the global oceans. *International Journal of Climatology*, **33**(8), 1936–1947, <https://doi.org/10.1002/joc.3562>.

Li, J. P., Q. C. Zeng, and J. F. Chou, 2000: Computational uncertainty principle in nonlinear ordinary differential equations (I)—Numerical results. *Science in China (Series E)*, **43**, 449–460, <https://doi.org/10.1360/ye2000-43-5-449>.

Li, X., R. Q. Ding, and J. P. Li, 2019: Determination of the backward predictability limit and its relationship with the forward predictability limit. *Adv. Atmos. Sci.*, **36**, 669–677, <https://doi.org/10.1007/s00376-019-8205-z>.

Li, X., R. Q. Ding, and J. P. Li, 2020a: Quantitative comparison of predictabilities of warm and cold events using the backward nonlinear local Lyapunov exponent method. *Adv. Atmos. Sci.*, **37**, 951–958, <https://doi.org/10.1007/s00376-020-2100-5>.

Li, X., R. Q. Ding, and J. P. Li, 2020b: Quantitative study of the relative effects of initial condition and model uncertainties on local predictability in a nonlinear dynamical system. *Chaos, Solitons & Fractals*, **139**, 110094, <https://doi.org/10.1016/j.chaos.2020.110094>.

Lorenz, E. N., 1963: Deterministic nonperiodic flow. *J. Atmos. Sci.*, **20**, 130–141, [https://doi.org/10.1175/1520-0469\(1963\)020<0130:DNF>2.0.CO;2](https://doi.org/10.1175/1520-0469(1963)020<0130:DNF>2.0.CO;2).

Lorenz, E. N., 1975: The physical bases of climate and climate modelling. *Climate Predictability*, **16**, 132–136.

Lorenz, E. N., 1989: Effects of analysis and model errors on routine weather forecasts. *Proc. ECMWF Seminar on Ten Years of Medium Range Weather Forecasting*, ECMWF, Reading, United Kingdom, 115–128.

Lorenz, E. N., 2005: A look at some details of the growth of initial uncertainties. *Tellus A*, **57**, 1–11, <https://doi.org/10.1111/j.1600-0870.2005.00095.x>.

Mintz, Y., 1968: Very long-term global integration of the primitive equations of atmospheric motion: An experiment in climate simulation. *Causes of Climatic Change*, D. E. Billings et al., Eds., Springer, 20–36, [https://doi.org/10.1007/978-1-935704-38-6\\_3](https://doi.org/10.1007/978-1-935704-38-6_3).

Mu, M., and W. S. Duan, 2003: A new approach to studying ENSO predictability: Conditional nonlinear optimal perturbation. *Chinese Science Bulletin*, **48**, 1045–1047, <https://doi.org/10.1007/BF03184224>.

Mu, M., and Z. Y. Zhang, 2006: Conditional nonlinear optimal perturbations of a two-dimensional quasigeostrophic model. *J. Atmos. Sci.*, **63**, 1587–1604, <https://doi.org/10.1175/JAS3703.1>.

Mu, M., W. S. Duan, and J. C. Wang, 2002: The predictability

problems in numerical weather and climate prediction. *Adv. Atmos. Sci.*, **19**, 191–204, <https://doi.org/10.1007/s00376-002-0016-x>.

Mu, M., W. S. Duan, and B. Wang, 2003: Conditional nonlinear optimal perturbation and its applications. *Nonlinear Processes in Geophysics*, **10**, 493–501, <https://doi.org/10.5194/npg-10-493-2003>.

Mukougawa, H., M. Kimoto, and S. Yoden, 1991: A relationship between local error growth and quasi-stationary states: Case study in the Lorenz system. *J. Atmos. Sci.*, **48**, 1231–1237, [https://doi.org/10.1175/1520-0469\(1991\)048<1231:ARBLEG>2.0.CO;2](https://doi.org/10.1175/1520-0469(1991)048<1231:ARBLEG>2.0.CO;2).

Nese, J. M., 1989: Quantifying local predictability in phase space. *Physica D: Nonlinear Phenomena*, **35**, 237–250, [https://doi.org/10.1016/0167-2789\(89\)90105-X](https://doi.org/10.1016/0167-2789(89)90105-X).

Oseledec, V. I., 1968: A multiplicative ergodic theorem. Characteristic Lyapunov exponents of dynamical systems. *Trans Moscow Math Soc*, **19**, 197–231.

Palmer, T. N., 1993: Extended-range atmospheric prediction and the Lorenz model. *Bull. Amer. Meteor. Soc.*, **74**, 49–66, [https://doi.org/10.1175/1520-0477\(1993\)074<0049:ERAPAT>2.0.CO;2](https://doi.org/10.1175/1520-0477(1993)074<0049:ERAPAT>2.0.CO;2).

Richardson, D. S., 1998: The relative effect of model and analysis differences on ECMWF and UKMO operational forecast. *Proc. ECMWF Workshop on Predictability*, ECMWF, Reading, United Kingdom, 363–372.

Sanz-Serna, J. M., and S. Larsson, 1993: Shadows, chaos, and saddles. *Applied Numerical Mathematics*, **13**(1–3), 181–190, [https://doi.org/10.1016/0168-9274\(93\)90141-D](https://doi.org/10.1016/0168-9274(93)90141-D).

Smagorinsky, J., 1969: Problems and promises of deterministic extended range forecasting. *Bull. Amer. Meteor. Soc.*, **50**, 286–312, <https://doi.org/10.1175/1520-0477-50.5.286>.

Trevisan, A., and R. Legnani, 1995: Transient error growth and local predictability: A study in the Lorenz system. *Tellus A*, **47**, 103–117, <https://doi.org/10.1175/JAS3824.1>.

Vallejo, J. C., and M. A. F. Sanjuán, 2013: Predictability of orbits in coupled systems through finite-time Lyapunov exponents. *New Journal of Physics*, **15**(11), 113064, <https://doi.org/10.1088/1367-2630/15/11/113064>.

Vallejo, J. C., and M. A. F. Sanjuán, 2015: The forecast of predictability for computed orbits in galactic models. *Monthly Notices of the Royal Astronomical Society*, **447**(4), 3797–3811, <https://doi.org/10.1093/mnras/stu2733>.

Vannitsem, S., and Z. Toth, 2002: Short-term dynamics of model errors. *J. Atmos. Sci.*, **59**, 2594–2604, [https://doi.org/10.1175/1520-0469\(2002\)059<2594:STDOME>2.0.CO;2](https://doi.org/10.1175/1520-0469(2002)059<2594:STDOME>2.0.CO;2).

Yoden, S., and M. Nomura, 1993: Finite-time Lyapunov stability analysis and its application to atmospheric predictability. *J. Atmos. Sci.*, **50**, 1531–1543, [https://doi.org/10.1175/1520-0469\(1993\)050<1531:FTLSAA>2.0.CO;2](https://doi.org/10.1175/1520-0469(1993)050<1531:FTLSAA>2.0.CO;2).